Contents lists available at ScienceDirect

Geotextiles and Geomembranes

Equivalent seismic coefficient in geocell retention systems

Dov Leshchinsky [a,*], Hoe I. Ling [b], Jui-Pin Wang [b], Arik Rosen [c], Yoshiyuki Mohri [d]

[a] Department of Civil and Environmental Engineering, University of Delaware, Newark, DE 19716, USA
[b] Department of Civil Engineering and Engineering Mechanics, Columbia University, New York City, NY 10025, USA
[c] PRS Mediterranean, Europe-Israel Tower, 2 Weizmann Street, Tel Aviv 64239, Israel
[d] National Research Institute of Rural Engineering, 2-1-6 Kannodai, Tsukuba City, Japan

ARTICLE INFO

ABSTRACT

Ideal design of an earthquake resistant earth structure would consider the time records of future seismic events. Objectively, such time records are difficult to predict especially when compared with prediction of the design peak ground acceleration (PGA), a single-value parameter. Furthermore, relevant soil properties are not easily obtainable in the field. Consequently, in routine stability designs, the state of practice utilizing a pseudostatic analysis has not changed for many years. To reduce the inherent conservatism of the pseudostatic approach, it is common to use a fraction of PGA in the stability analysis. For earth structures such as slopes, existing standards suggest a value of this fraction, typically varying between 0.3 and 0.5 times PGA. While one hopes that such values are calibrated against case histories, it is doubtful if there is sufficient field data for a value corresponding to geocell gravity walls and geocell reinforced slopes. Reported here are relevant results of shake table tests on five different geocell structures, each 2.8 m high, subjected to an excitation simulating the Kobe earthquake. Exhumation enabled the tracing of slip surfaces that developed during the shaking. Back-analysis resulted in the fraction of the applied PGA needed to establish a slip surface. The formation of slip surfaces in the context of this work should not be interpreted as collapse or catastrophic failure; rather it signifies the development of an active wedge. Hence, the equivalent coefficients in this work are an upper bound value for the magnitude and intensity of the ground motion applied in the analysis. It was found that for geocell gravity walls, essentially flexible structures, the upper bound seismic coefficient for the applied motion is about 0.4 times PGA. For reinforced geocell walls the upper bound coefficient would be 0.3 times PGA.

© 2008 Elsevier Ltd. All rights reserved.

1. Introduction

Design of slopes is typically based on limit equilibrium (LE) stability analysis. Pseudostatic slope stability analysis assumes an equivalent seismic coefficient, typically in the horizontal direction, which results in additional force components in the limit equilibrium equations, all proportional to gravity. Specifying the seismic coefficient as peak ground acceleration (PGA) is likely overly conservative as it considers the maximum seismic forces permanent rather than momentary. This statement assumes that liquefaction is not an issue as it is unrelated to the LE analysis. It also assumes that potential strength degradation of the soil is already considered in specifying the design strength parameters.

The ideal approach to design any structure subjected to earthquake loading is based on tolerable recoverable and/or permanent displacements. The simplest approach is the well-known "stick–slip" method by Newmark (1965). While Newmark's approach is simple to apply, it is not clear how it could be applied when considering the reinforcement. Generally, there are several difficulties in applying any displacement approach. First, the soil relevant properties under dynamic loading need to be characterized with reasonable accuracy to obtain reliable displacements. Second, the *full* record of a design earthquake needs to be known *before* such an earthquake takes place. Accurate prediction of such a record is not yet feasible since it is highly random. Third, to render accurate predictions, a numerical tool that can accurately replicate soil seismic behavior is needed. It is not clear whether such a tool is readily available for common design of slopes. Fourth, design codes may not define what a tolerable displacement of a slope is. Hence, the 'acceptable value of displacement' issue is considered as an 'engineering judgment' meaning that the outcome is subjective. For example, as displacement is not uniform, one may ask where on the structure's surface the displacement criterion should be applied. Subjective design criterion limits the value of a potential gain in accuracy. Clearly, the state-of-the-art in seismic slope stability analysis is not yet sufficiently developed so as to entirely replace the current design practice.

* Corresponding author.
  E-mail address: dov@udel.edu (D. Leshchinsky).

The alternative approach of a pseudostatic analysis utilizes the anticipated PGA, a_{max}. While this value (*number*) is also random, it is much easier to estimate the PGA than the full time record of an earthquake which is a random *function*. In fact, many codes provide the PGA based on location and historical data. However, direct use of the PGA in design implies unrealistic large pseudo-inertia forces, often rendering seismic design uneconomical. As an example, FHWA (2001) requires the use of the full value of PGA combined with factor of safety greater than 1.0 when designing reinforced walls. To overcome the over-conservatism associated with specifying a_{max} in design, a fraction of a_{max} may be used in conjunction with a pseudostatic LE analysis. The factor of safety in such LE analysis needs to be a little larger than 1.0, preferably related to the ramifications of failure. Kramer (1996) presents an overview and discussion on the selection of the pseudostatic coefficient in design. For example, Kramer (1996) provides a reference to the work by Hynes-Griffin and Franklin (1984) in which it is recommended to use a design horizontal coefficient ratio of $a/g = (a_{max}/g)/2$ where a_{max} is the free field peak ground acceleration at the site. This recommendation is based upon acceptable deformations of up to 1 m. A report issued by IITK (2005) for seismic design of dams and embankments suggests using $a/g = (a_{max}/g)/3$ provided a_{max} or PGA is the acceleration at the toe elevation.

While design guidelines provide recommendations for ordinary slopes, the information available for the coefficient of steep slopes is limited. Ashford and Sitar (2002) presented a rational seismic approach for steep slopes. However, it is applicable for cemented soils rendering brittle slopes. Unlike cemented soils, geocell slopes and geosynthetic reinforced steep slopes are ductile and flexible. Therefore, such structures are likely to be more effective than ordinary slopes under seismic loading. FHWA (2001) essentially suggests that Hynes-Griffin and Franklin (1984) value should be used for reinforced steep slopes. The authors could not identify seismic guidelines for geocell slopes or walls.

An ideal approach would be to consider field data of seismic induced instability and combine it with the excitation record to back-calculate the equivalent seismic coefficient. In LE analysis, a complete verification also needs to include a check of the predicted and the actual slip surfaces. Such data, however, is a "luxury" since the soil properties and trace of critical slip surface in the field, especially, are rarely known. This is even rarer with seismic failure of reinforced slopes; in actuality, there is very limited comprehensive data for failure of such structures even under static loading. This work presents results of carefully controlled tests where a Kobe earthquake record, released by Japan Meteorological Agency, was used to induce "failure" of carefully constructed geocell slopes.

It should be noted that the objective of testing the geocell slopes was to study the behavior of such systems under seismic conditions. Upon examining the results, however, it became clear that a byproduct of this objective would be an addition to the limited database on the equivalent pseudostatic seismic coefficient. Consequently, this paper is focused on reporting the empirical, directly assessed, seismic coefficients in the tested models.

2. Tests

Technical details of the large shake table utilized in this test program are described in Ling et al. (2005). This shake table is located at the Japan National Research Institute of Agricultural Engineering, Tsukuba City, and it can excite gross maximum payload of 500 kN (net 360 kN) to vertical and/or horizontal acceleration of 1g. The metal testing box containing the reinforced slopes was 2 m wide, 6 m long and 3 m tall. To minimize reflection of waves from the side and rear of the metal box, expanded polystyrene (EPS) boards, 5 cm thick, were placed against the testing box walls. To reduce friction with the sidewalls, greased plastic sheeting was placed against EPS. The observed slip surfaces at the crest extended from side to side of the box indicating minimal end effects. Furthermore, outward displacements at each elevation were nearly uniform and the crest settlement was nearly uniform at each transverse section again implying that end effects were minimal. Hence, 2-D behavior was likely simulated.

In all tests, an attempt to apply a record of the 1995 Kobe earthquake was made. The Kobe record used is displayed in Fig. 1. This record includes the horizontal acceleration (NS = North–South and EW = East–West) and the vertical acceleration (UD = Up–Down). The vector component of the PGA in the NS was 0.59g, in EW it was 0.63g, and UD it was 0.34g. Note that the peak vertical acceleration did not occur simultaneously with the peak horizontal acceleration.

The shaking table 2-D loading in all tests included the time record of NS and UD. While the time record can be applied with high level of accuracy, the amplitude generated by the hydraulic actuator is difficult to achieve accurately. The amplitude or the acceleration is dependent mainly on the payload and several calibration tests are needed so that setting of the shaker's control can render accurate amplitude. The alternative of achieving precise digital control of amplitude via feedback from mounted accelerometers is technically difficult when considering the rate of load application and the weight of the tested model. Consequently, the actuators were adjusted before each excitation with the expectation that the induced "ground motion" amplitude would be close to the target value. The "actuators" in the context of these tests mean the actuator generating the horizontal motion and the actuator generating the vertical motion both applied at the base of the shake table box.
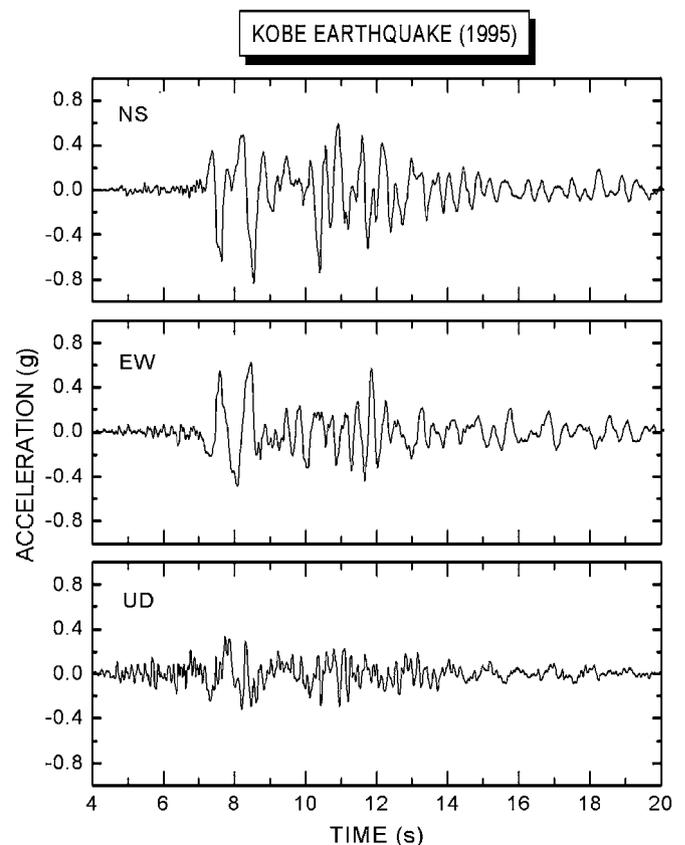

Fig. 1. Time record from Kobe earthquake applied in tests (NS = North–South; EW = East–West; UD = Up–Down).

In Tests 1 and 3, the excitation was applied in two stages. The target excitation was attenuated horizontal acceleration amplitude of PGA = 0.4g and vertical PGA = 0.2g. Following a relaxation period of about 1 h, the target excitation amplitude in the second stage was amplified horizontal acceleration of PGA = 0.8g and vertical PGA = 0.4g. In Tests 2, 4 and 5, three loading stages were used: target horizontal acceleration PGA = 0.4, 0.8g, and the shaker maximum capacity for the given payload, 1.2g, for the first, second and third loading stage, respectively. The target vertical acceleration was for PGA = 0.2, 0.4 and 0.5g for the first, second and third loading stage, respectively. The relaxation period between each excitation in Tests 2, 4 and 5 was about 1 h. Table 1 shows the applied PGA as recorded by accelerometers installed on the base of the table. Clearly, the field-recorded value was not achieved; there was a significant overshoot in horizontal PGA at the second and third loading stages thus reflecting larger earthquake intensity than the record shown in Fig. 1. It should be noted that in Fig. 1 and Table 1 the horizontal PGA is in the outwards direction; the vertical PGA is in the upwards acceleration.

Five tests were conducted. All tested slopes, except for Test 5, were 2.8 m high, resting on a 0.2 m thick foundation soil. The slope in Test 5 was 2.7 m high since the reinforcement used, 0.05 m thick geocell reinforcement, could not result in exactly 2.80 m height. The geocells, resembling a honeycomb structure, were 0.2 m high with internal aperture of approximately 0.21 m by 0.21 m. The geocell was fabricated by PRS Mediterranean using sheets of HDPE welded to form a regular pattern of cells. Fourteen geocell layers were placed on top of each other with an offset of about 0.1 m to form the face of the slope. This offset translates into an average face inclination of 2(v):1(h) or 63.4°. The top geocell layer was 2.52 m long, much longer than all layers below. This top layer was infilled with compacted gravel. Prior to the tests, it was postulated that long top layer made of geocell will inhibit crack or even slip surface formation immediately below this layer. While numerous small, mainly shallow, tension cracks initiated at the soil surface away from the top layer, none was observed immediately below in any of the five tests.

Fig. 2 shows the geocell layout in each of the five tests. As seen, Tests 1 and 3 have the same general configuration. In Test 1, however, the cells are infilled with compacted gravel whereas in Test 3 the cells are infilled with the same fine sand comprising the slope. Tests 1 and 3 can be considered as flexible "gravity walls". However, since the geocell is infilled with soil, it can be considered as a composite material. The authors prefer to categorize it as a reinforced slope where the facing units are made of reinforced soil. In fact, as per the FHWA (2001) definition, a wall has batter less than 20° while the tested structure had a batter of 26.6°. Hence, the categorization as slope is compatible with common notation.

Tests 2, 4 and 5 had their front geocell facing made up of only three cells each (0.63 cm deep). In Test 2 the infill material was gravel whereas in Test 4 it was infilled with the same sand as the backfill material. Geogrid layers, 1.8 m total length (i.e., extending 1.17 m beyond the back of the facing) and spaced no more than

0.4 m apart (Fig. 2), were installed in Test 2. Test 4 included three geocell layers that were 1.68 m long (eight cells), extending into the backfill. The extended geocells were infilled with sand, same as all other geocells forming the facing, except for the top layer. Since the bottom extended layer was placed over the foundation soil serving as a base for the wall system, there were effectively only two extended geocell layers reinforcing the backfill, spaced 0.6 and 0.8 m apart. Test 5 was comprised of six geocell layers, 0.05 m high, each having a total length of 1.84 (i.e., extending 1.21 m behind the back of the facing). The three cells confined between stacked facing units (Fig. 2) were infilled with gravel while the other six cells, embedded within the reinforced soil, were infilled with the same sand as the reinforced soil. Except for the bottom, spacing was 0.4 m. Considering the heights of geocell layers, the weight of reinforcement in Test 5 is nearly half of that in Test 4. Such a layout is economical to use as a reinforced slope system made entirely of geocell material. Test 5 is approximately equivalent to Test 2 where geogrid rather than 0.05 m high cells was used as reinforcement. While geogrid is essentially a planar reinforcement, geocell (even 0.05 m) serves as a 3-D reinforcing element. It should be noted that a potential problem in using geocell material for reinforcement of sizeable structures is the low long-term tensile strength of the HDPE polymer. As tested, long-term strength accounting for creep was not an issue as virgin HDPE material was subjected to short static and seismic loading period.

Tests 2, 4 and 5 represent the practical minimal thickness of facing while reinforcement is embedded as horizontal discrete polymeric material in the backfill. That is, while Tests 1 and 3 represent gravity structures which could be economical for limited height, Tests 2, 4 and 5 represent potentially economical reinforced slopes that could be tall. Long-term issues related to the selection of reinforcement (e.g., creep, durability) and the exposed facing (e.g., UV degradation, thermal expansion) are not discussed here.

The backfill soil behind the facing and in the 0.2 m thick foundation was fine uniform sand (D_{50} = 0.27 mm; 0.35% passing sieve #200; Cu = 2). Standard Proctor compaction tests indicate that the maximum dry unit weight is 15 kN/m^3 and the optimal moisture content of 16%. The backfill was compacted to 90% of Standard Proctor at a moisture content of 16% yielding a dry unit weight of 13.5 kN/m^3 or moist unit weight of 15.6 kN/m^3. Compaction was done by a hand-held vibratory compactor. Drained triaxial tests were conducted on three specimens compacted to the same density as in the tested walls; these tests were at confining pressures of 40, 70, and 100 kPa. The Mohr–Coulomb failure envelop yielded a peak strength of $\varphi = 38°$ with no measurable apparent cohesion. However, tension cracks that formed at the crest during the shaking imply that there was a trace of cohesion, likely due to capillary tension or suction. Small apparent cohesion may increase stability and thus lead to overly optimistic results related to stability. However, based on observations during the tests, the active wedge formed instantly at the second or third excitation loading stage. Once formed, the capillary tension, and possible apparent cohesion, vanishes at the slip surface thus leading to acceptable back-analysis and conclusions where the cohesion is taken as zero. To avoid the issue of potential apparent cohesion, a legitimate procedure to prepare the model would have been to compact the fine sand dry. The tradeoff to such procedure is a more difficult compaction, which aims at achieving a prescribed and consistent value of unit weight, done in the difficult environment of the testing box. More importantly, exhumation where the location of the slip surface is traced (as done in this work) would have required significantly more resources as the level of sophistication for such measurement by far exceeds that of using embedded colored sand seam.

The unit weight of the compacted gravel was 19.9 kN/m^3. The polyester geogrid used in Test 2 had an ultimate strength of 35 kN/m, exceeding the needed strength. Ling et al. (in press) provide

Table 1
Applied PGA

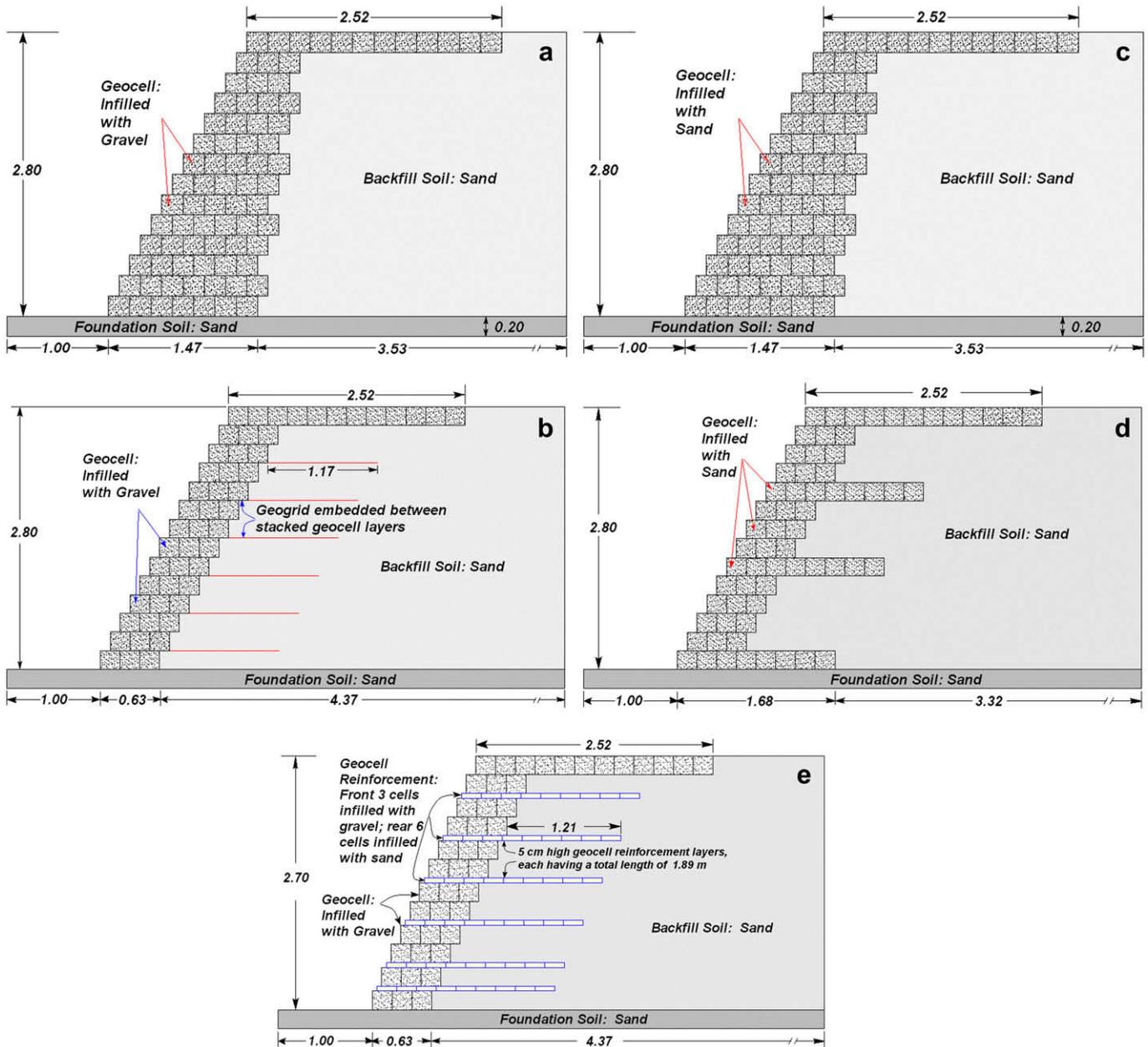| Recorded PGA in field (Fig. 1)	Test	Applied peak acceleration at base of shake table					
		Horizontal PGA at each loading stage (g)			Vertical PGA at each loading stage (g)		
		1	2	3	1	2	3
Horizontal: 0.59g, vertical: 0.34g	1	0.46	0.92	N/A	0.21	0.42	N/A
	2	0.46	0.94	1.21	0.20	0.39	0.47
	3	0.48	0.94	N/A	0.20	0.39	N/A
	4	0.47	0.95	1.22	0.20	0.37	0.48
	5	0.41	0.87	1.21	0.18	0.34	0.50

Fig. 2. Configuration of tested systems (length in meters). (a) Test 1: no reinforcement and gravel infilled geocell. (b) Test 2: geogrid reinforcement and gravel infilled geocell. (c) Test 3: no reinforcement and sand infilled geocell. (d) Test 4: geocell reinforcement infilled with sand. (e) Test 5: geocell reinforcement infilled with sand while geocell facing infilled with gravel.

more details about the backfill sand and the geogrid as well as instrumentation and details of results that are not directly relevant to this work.

White thin seams of sand were placed every about 0.4 m within the backfill material. Upon completion of each test, the slope was carefully excavated to observe dislocations of these seams so that traces of slip surfaces could be identified. The slopes were heavily instrumented; however, this instrumentation is not relevant to the current paper.

3. Results

Accelerometers embedded within the backfill soil and facing, at several elevations, indicate that magnification of base acceleration was negligibly small (less than 1.2), typically showing a small attenuation along the height (Ling et al., in press). This is perhaps not

a surprise with flexible earth structures as they deform during a shaking, dissipating energy and acting, de facto, as shock absorbers or dampers. It implies that the recorded results are likely applicable to taller slopes than those tested. However, the question as to what is the limit for a tall slope, where its damping is too small to prevent large amplification as the excitation frequency approaches its resonance, cannot be answered here explicitly as it requires an extrapolation of the current work. A suitable numerical analysis is a more practical tool to address this question. Based on tests' observations and recorded data (mainly attenuation), the authors believe that a slope twice as high as the tested ones would still have small amplification.

It should be noted that in this work, the equivalent seismic coefficient is configured with respect to the applied horizontal PGA, as this is the value typically used in design codes. However, the recorded performance was generated by a combined horizontal

and vertical accelerations and therefore, the resulted equivalent seismic coefficients are likely to be conservative as it attributes all to the horizontal excitation.

To find the equivalent seismic coefficient, it is convenient to define seismic reduction factor, RFs = a/PGA, where a is the equivalent seismic coefficient (i.e., a is the design pseudostatic seismic coefficient). In this work, the seismic reduction factor, RFs, for each test was determined using the recorded PGA that caused an active wedge to develop combined with an adequate pseudostatic limit equilibrium analysis of each problem. In limit equilibrium design, one would employ a(=RFs × PGA) to obtain adequate seismic stability; i.e., adequate factor of safety, Fs, under pseudostatic conditions (typically this Fs is about 1.1 whereas the static one is 1.3–1.5).

3.1. Tests 1 and 3

As noted before, the difference between these two tests is the infill material in the geocells. In Test 1 it was compacted gravel (with estimated strength of φ in excess of 45°) whereas in Test 3 the infill was the same sand as the backfill ($\varphi = 38°$). In the stability analysis used for reducing the data the exact feasible value of φ for the gravel has little impact on the results as long as it is larger than 40°.

Following the last excitation in Test 1, excavation revealed that no fully developed slip surface could be observed through the section. Only some shallow dislocations of the thin white sand layer occurred behind the top geocell layer. The outward maximum permanent displacement of the facing and the crest maximum settlement were 31 and 27 mm, respectively (Table 2). Conversely, in Test 3 the outward maximum permanent displacement of the facing and the crest settlement were 47 and 40 mm, respectively (Table 2). Furthermore, in Test 3 excavation showed a clear trace of a slip surface through the section – Fig. 3. Note that this surface appears to represent a translational movement where the surface emerges between the second and third layer of geocells. That is, the trace of the slip surface in Fig. 3 terminates at the rear end of the facing at about 0.4 m above the foundation. Note that the geocell seen in Fig. 3 was trimmed during excavation to allow for a better view of the facing panels. The geometry of the sliding mass appears to be that of a wedge. It should be emphasized that the observed slip surface was not associated with what one would consider as catastrophic failure or collapse. This surface reflects a rather small movement of the face due to severe seismic loading, perhaps indicating an active state of stresses.

Under static loading, a two-part wedge analysis using program ReSSA(2.0) (Leshchinsky and Han, 2004) yields for Test 1 a factor of safety, Fs, of 1.99 and for Test 3, 1.89. The trace of the slip surface for either case is similar (see Fig. 4), emerging at the interface between the lower geocell and the foundation soil. Along this interface the friction angle is that of the sand ($\varphi = 38°$). Test 1 yields slightly larger Fs because the weight of the infilled geocells with gravel (Test 1) is somewhat larger than the weight when infilled with sand (Test 3) thus the interface frictional shear resistance along the geocell–sand increases.

A pseudostatic stability analysis on Test 1 indicates that at an acceleration of about 0.35g, Fs is 1.00. The applied horizontal PGA for Test 1 rendering Fs = 1.00 was about 0.92g – see Table 1. Consequently, for Test 1 it can be stated that the value of the seismic reduction factor, RFs, is 0.35/0.92 = 0.38. For comparison with other tests, Table 3 presents the reduction factors, RFs, for all tests. Note that in Test 1 no slip surface was fully developed. Furthermore, the pseudostatic analysis used considered only horizontal coefficient whereas in reality there was also some vertical component. It is noted that large vertical acceleration combined with large horizontal acceleration may decrease stability significantly (e.g., Ling and Leshchinsky, 1998). However, it is customary in design to consider the horizontal acceleration only, perhaps based on the belief that the vertical and horizontal accelerations will not peak simultaneously. Hence, the 'calibration' in this work followed the customary design approach. It is also noted that the initial shaking at PGA of 0.46g likely loosened the soil (i.e., settlement developed on the crest while the wall moved outwards thus increasing slightly the overall volume of the soil in the model box) thus degrading slightly the strength. Hence, RFs is likely smaller than 0.38. However, the measured data do not permit quantification of this statement.

Fig. 5 shows the safety map for the pseudostatic analysis of Test 3 considering a two-part wedge mechanism combined with Spencer Method. The safety map (Baker and Leshchinsky, 2001) is a powerful diagnostic tool for the state of stability of a slope. Observing Fig. 5, one sees that sliding could occur along the interface with the foundation or between the second and first geocell layers or between the third or second geocell layers. For all these three surfaces the safety factor varies between 1.00 and 1.03, practically the same value. Comparing the critical slip surface observed in Fig. 3 and the predicted pseudostatic slip surface in Fig. 5, one sees good agreement.

In Test 3, the equivalent seismic coefficient is 0.35g whereas a fully developed slip surface (Fig. 3) was realized at an excitation PGA of 0.94g using a Kobe earthquake record. Subsequently, the upper value for the seismic reduction factor, RFs, is 0.35/0.94 = 0.37. To get collapse and not just a clearly defined slip surface, however, the induced PGA should have been larger than 0.94g. It can be stated that the equivalent pseudostatic coefficient for gravity geocell walls supporting sand backfill should be less than 0.37 times PGA. Compared with the recommended value of 0.5 for geosynthetic reinforced slopes in FHWA (2001), the value of 0.37 represents about 25% reduction.

As a side note, the seismic reduction factor leading to "failure" in Tests 1 and 3 is computationally the same ($a/g \cong 0.37$). This is somewhat misleading as in Test 1 there was no observed slip surface. Furthermore, up to PGA of 0.92, the measured performance of Test 1 was better than that of Test 3. In the analysis this is due to the bottom geocell layer resting on the foundation soil. That is, the interface at the bottom elevation is controlled by the strength of the sand and not the gravel that infills the cells. In reality, the lower geocell layer will be embedded in the foundation soil. Such a constraint will eliminate a "weak" frictional interface between the lower geocell and the soil surface at the toe grade elevation. In such a case, the resulted Fs from analysis will be higher than obtained here and the benefit of using gravel as infill will be realized.

3.2. Tests 2, 4 and 5

In Test 2 geogrid layers were used (Fig. 2). To increase the strength of the frictional connection between the geogrid and confining geocell layers, compacted gravel was used as an infill in the geocells. In Test 4 the infill was the same sand as the backfill ($\varphi = 38°$) and three layers of geocell were extended into the backfill. In Test 5, six layers of 0.05 m high geocell layers were used as

Table 2
Measured maximum displacements

Test	Maximum permanent displacement of face (mm)	Maximum settlement of crest (mm)
1	31	27
3	47	40
2	95	115
4	150	150
5	95	85

Note: Measured values for Tests 1 and 3 were at about PGA = 0.93g. For Tests 2, 4 and 5 measured values were at about PGA = 1.21g.
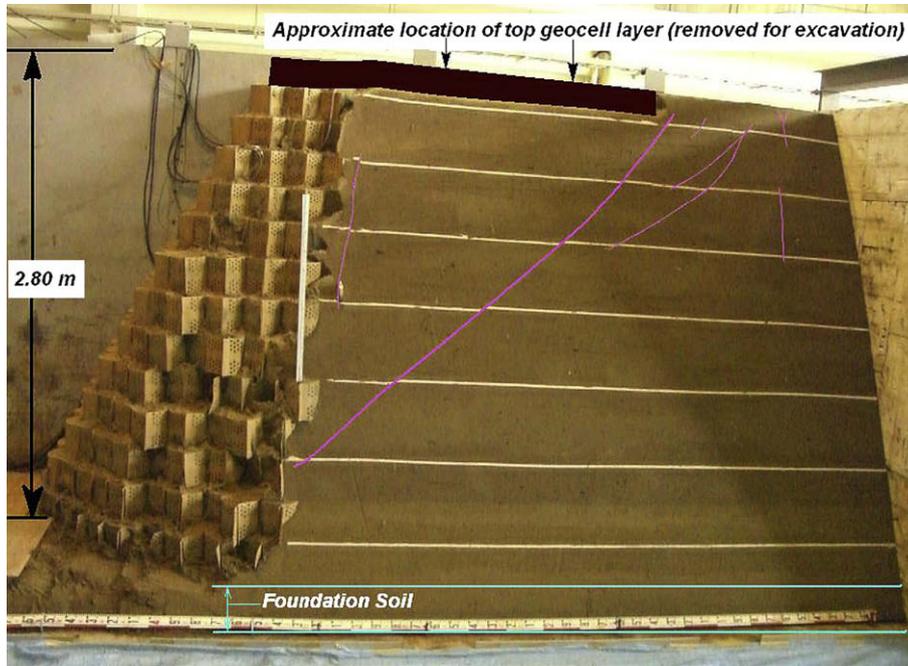
Fig. 3. Excavated section: Test 3 (PGA = 159% of Kobe's).

reinforcement (approximately similar layout as the geogrid layers in Test 2). The geocell portion embedded between the stacked facing units was infilled with gravel while the reinforcing portion was infilled with the same sand as the reinforced soil.

Post-excitation excavation of Test 2 (PGA = 1.21g) revealed only some shallow discontinuities next to the soil surface, behind the top geocell layer. No continuous slip surface was observed. The maximum facing outward permanent movement and crest settlement during the third shaking were about 95 and 115 mm, respectively, for Test 2 (Table 2). In Test 4, the maximum movements were 150 and 150 mm for outward and settlement displacements, respectively (Table 2). In Test 4 a trace of slip surface was fully evolved through the section – Fig. 6. Looking at the bending of the extended geocell layers and the geometry of the slip surface, it appears that rotational slip surface developed, tending to emerge above the bottom geocell layer. A circular arc would seem to fit this failure well. However, the appearance of a fully developed slip surface was not associated with catastrophic collapse, just a small translation and rotation under extreme PGA of 1.21g, 205% of the Kobe's maximum horizontal acceleration.
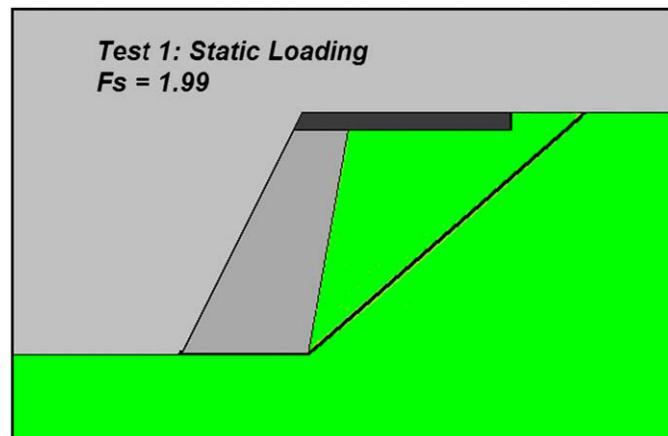
Under static loading, Bishop Analysis (circular arc) yielded for Test 2 an Fs = 1.85 and for Test 4, Fs = 1.61. For translational analysis (two-part wedge) using Spencer's Method, Fs = 2.07 for Test 2 and 2.14 for Test 4. Limit equilibrium analysis for the model configuration employed in Test 2 combined with a seismic coefficient of 0.39, the Fs for rotational failure was 0.97 and for translational failure Fs was 0.98, practically the same value. The critical traces are shown in Fig. 7.

Fig. 7 indicates that the computed pseudostatic seismic coefficient needed to generate failure is less than 0.39. Consequently, for Test 2 it can be stated that the upper value of the seismic reduction factor, RFs, is 0.39/1.21 = 0.32. It should be pointed out that the initial shaking at PGA of 0.46g and subsequently at 0.94g may have degraded the soil strength. Hence, the RFs is likely be smaller than 0.32.

Under acceleration of 0.3g in Test 4, the calculated Fs for translational failure is about 1.15 and for rotational failure it is 0.99. Fig. 8 shows the critical slip circle for the pseudostatic analysis of Test 4 considering rotational failure mechanism combined with Bishop Method. Comparing the trace of the surface in Fig. 8 with the measured trace in Fig. 6, one can see that the computed trace resembles well with the measured one.

In Test 4, seismic coefficient of 0.30g yielded "failure" in the pseudostatic analysis whereas a continuous slip surface developed at PGA of 1.22g – Fig. 6. Subsequently, the upper value for the seismic reduction factor, RFs, is 0.30/1.22 = 0.25. To render catastrophic collapse, however, the induced PGA should have been larger than 1.22g. For this reason and since Test 2 was not yet at failure, it can be stated that RFs for the reinforced geocell slope

Fig. 4. Two-part wedge using Spencer Method (static loading).

Table 3
Summary: calculated seismic reduction factors

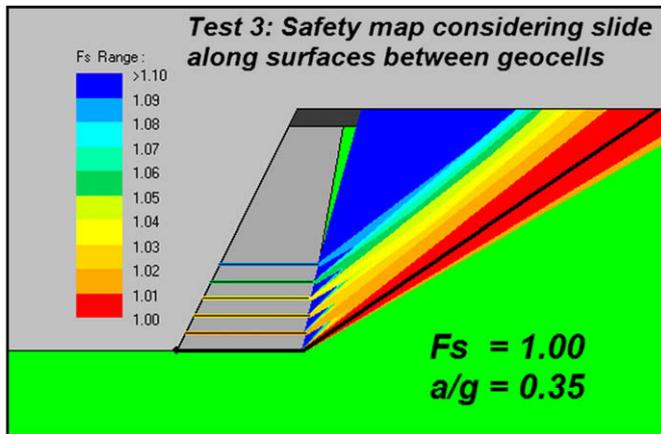| Test	Seismic reduction factor (RFs = a/PGA)
1	0.38
3	0.37
2	0.32
4	0.25
5	0.25

Fig. 5. Safety map for Test 3 using Spencer analysis: pseudostatic loading.

should be about 0.25. For this RFs, the resulted displacement would be rather small (see Table 2). Compared with the recommended value of 0.5 for geosynthetic reinforced slopes in FHWA (2001), the value of 0.25 represents a 50% reduction.

Test 5 deserves special attention. Observing Fig. 9 one sees two continuous rotational slip surfaces. It is likely that the shallower one developed first while the deeper one is a secondary failure as shaking continues. In particular, the shallower surface passes through some (four) geocell reinforcement layer. It means that the 0.05 m high geocell reinforcement deformed and bent sufficiently to allow for the slip surface to propagate. This indicates that the geocell reinforcement is effective in its contribution to stability (i.e., not excessively strong and obviously not too weak).

Back-analysis of Test 5 as done in the other four tests cannot be done without some speculation since the mobilized strength of the geocell is not precisely known. However, postulating that the pseudostatic failure acceleration would be similar to that of Test 4 (i.e., about 0.30g) and using ReSSA to calculate the required strength of the geocell to achieve the same failure acceleration, one gets about 4 kN/m. The slip surface predicted by ReSSA is similar to the shallow surface in Fig. 9 – see Fig. 10. Note that for simplicity the geocell layers in ReSSA (Fig. 10) were considered planer with the

capacity to produce the prescribed tensile resistance or be pulled out, whichever is smaller. How reasonable is a mobilized strength value of 4 kN/m for a low stiffness of HDPE made of 0.05 m high welded strips? In an unrelated work, tensile tests conducted in a commercial laboratory on a similar geocell structure indicate that at about 5% elongation, the corresponding tensile force per unit width of welded strips forming the geocell structure would be about 4 kN/m. Elongation of about 5% should be sufficient to allow the formation of a continuous slip surface (i.e., active wedge) in the medium-dense sand used in Test 5. Consequently, the postulated pseudostatic acceleration in Test 5 equal to that of Test 4 yields reasonable tensile reaction in the reinforcement thus implying that the assumed acceleration is reasonable. That is, it yielded both a slip surface that agrees with that of Test 5 (see Figs. 9 and 10) and mobilized tensile resistance in the geocell that agrees with laboratory short-term test results. "Computed" seismic coefficient of 0.3g for Test 5, whereas the applied PGA was 1.21g, results in a seismic reduction factor, RFs, of $0.3/1.21 = 0.25$.

It should be noted that the maximum outward permanent movement of the facing and maximum crest settlement during the third shaking were about 95 and 85 mm, respectively. The corresponding numbers for Tests 2 and 4 were about 95 and 150 mm for the maximum outward movement, and about 115 and 150 mm for the settlements. The maximum movement of the facing in all tests occurred at about 0.5 m below the crest. Near the toe the outward movement was small, a few millimeters only. Maximum settlement occurred away from the facing. While the measured maximum movements under rather than high excitation of about 1.2g horizontal PGA are substantial, up to 5% of the height, there was no collapse in either case. Overall, Test 5 yielded the lowest maximum outward movement of the facing with slightly larger movements in the lower portion when compared with Test 2. The formation of a slip surface through the geocell reinforcement in Test 5 indicates that the system of soil-reinforcement is efficient as both the soil shear strength and the geocell tensile resistance are mobilized thus contributing to the stability of the flexible structure.

4. Observations

Recall that all tests were subjected to horizontal PGA that was either about 160 or 207% of the Kobe's earthquake. Although a complete slip surface was observed within the soil mass in Tests 2,
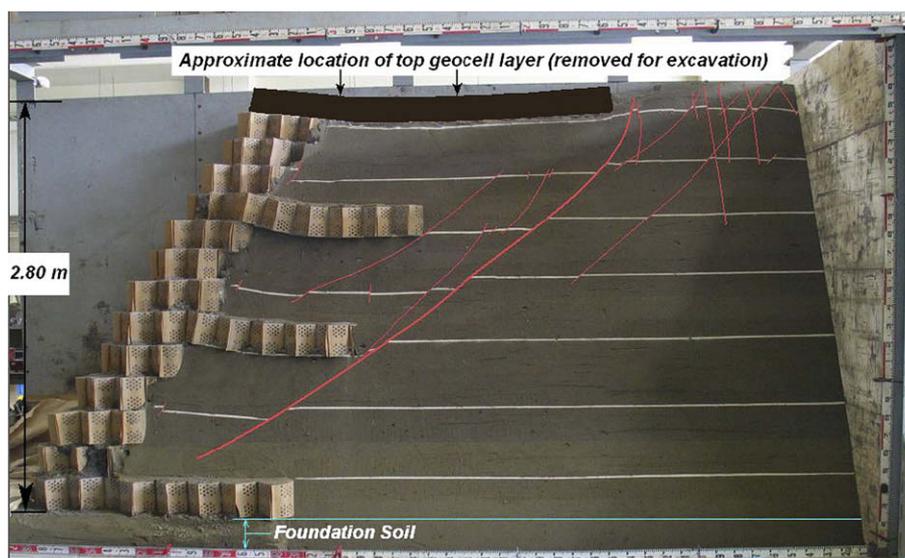

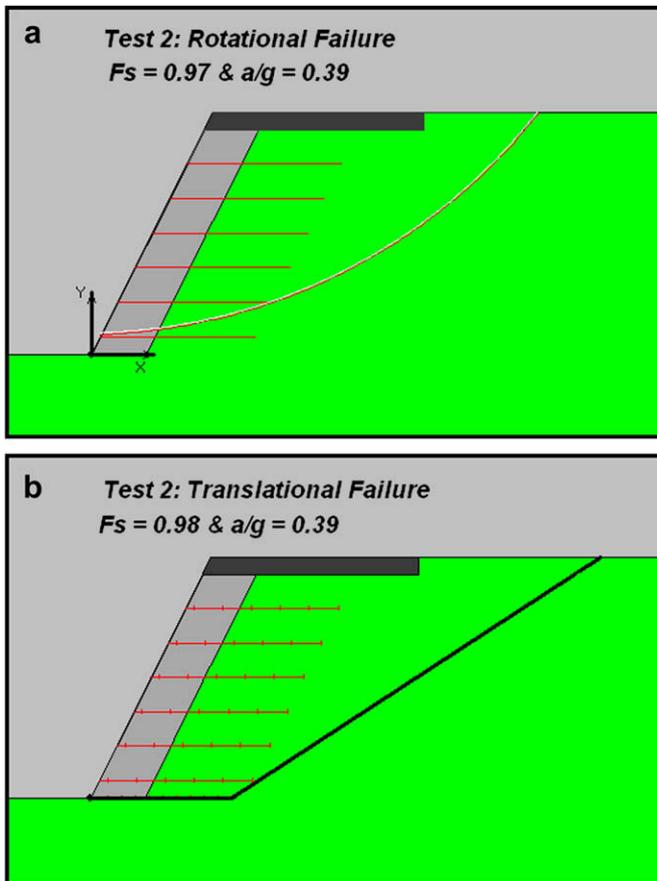**Fig. 6.** Excavated section: Test 4 (PGA = 205% of Kobe's).

Fig. 7. Critical slip surfaces for Test 2 under seismic loading. (a) Rotational failure. (b) Translational failure.

4 and 5, the functionality of the reinforced system was not significantly hindered. There was some deformation of the facing, a small vertical settlement of the geocell mattress on top, and shallow cracks developed behind this mattress (e.g., Figs. 3 and 6 – depth of cracks was about 50 cm). To complement the section through the shaken model shown in Fig. 3 (Test 3), the post-test frontal view of the same slope is shown in Fig. 11. Clearly, the development of a slip surface in the context of the tests is to a large extent analogous to the development of an active state of static stresses in classical earth pressure theories. The fact is that retaining walls are designed based on this state. Hence, the categorization here does not mean
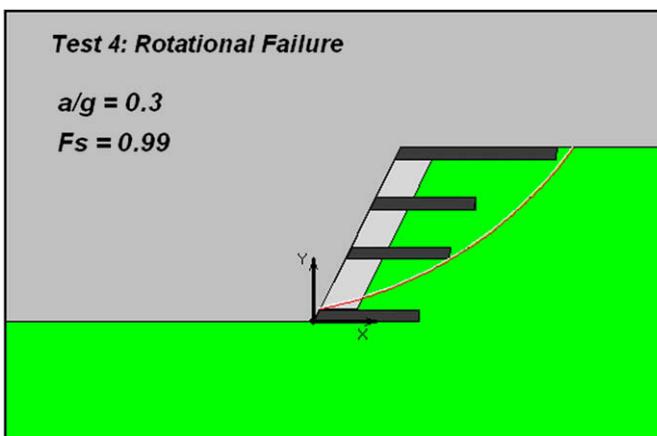

Fig. 8. Predicted critical slip circle for Test 4.

collapse but rather a situation in which the soil fully contributes its strength.

The geocell wall in Fig. 11 (Test 3) was not designed to withstand substantial seismic load considering established design criteria for gravity walls. This is obvious when one looks at its base to height ratio being only about 0.5, considering it has a front batter of 2(v):1(h) and it is infilled with soil which makes the wall lighter than the alternative conventional concrete gravity wall. The unexpected seismic performance of the gravity geocell wall may be attributed to the following features of the tested system:

1. Facing flexibility: this allows for dissipation of energy and for load shedding that results in lower load intensity on the facing as well as a seismic load resultant that is lower than in rigid walls.
2. Interaction of geocell layers: the small relative movement between geocell layers allows for energy dissipation via friction while maintaining limited translational movement between layers. This is due to high friction between adjacent layers and strong interaction of the infill material within the HDPE cells. The observation regarding the impact of sliding resistance between geocell layers is also supported by the difference between Tests 1 and 3. That is, in Test 1 the infill is gravel thus rendering higher stability than Test 3 where the infill is sand.
3. Long top layer: the long mattress of geocell placed as a top layer (see Figs. 3 and 6) inhibits the initiation of slip surfaces immediately below it. Slip surfaces initiated behind that mattress. 'Pushing back' the critical slip surfaces exerts smaller loads on the facing or into the reinforcement when compared with a case where the slip surface is free to develop anywhere (i.e., without long top mattress). Consequently, the geocell facing needs to resist lower loads as the potential failures are 'pushed' back to form less 'critical' active wedge thus increasing the stability of the system. Furthermore, reduced loads also result in smaller deformations thus producing better performance of the system even if stability is not an issue.

There was no reported failure of any geosynthetic reinforced wall in the Kobe earthquake (Tatsuoka et al., 1995). Hence, it is not possible to make a direct comparison between the reinforced walls in Kobe and Tests 2, 4 or 5. However, it can be stated that in any case, the performance of the reinforced systems was very good. Kobe's reinforced wall performance and the observations in this work mutually support each other.

5. Concluding remarks

Current practice of designing reinforced or unreinforced slopes and walls is to identify the local PGA and use a fraction of it in a pseudostatic analysis. This fraction is the reduction factor for pseudostatic analysis. The Kobe earthquake was used as a reference for an excitation to identify this coefficient. It is likely that if another excitation was used, the reduction factor would be different. However, the Kobe earthquake was significant in terms of damage to slopes and walls thus qualifying it to serve as a good reference for calibrating this reduction factor and the associated seismic coefficient. Seismic coefficients and reduction factors for pseudostatic limit equilibrium analyses are used in design codes worldwide.

Results obtained from a large scale shake table tests on reinforced geocell slopes are presented. These results are compared with a pseudostatic limit equilibrium analysis. The predicted failure mechanisms are similar to those observed in the tested slopes. However, the seismic coefficients required to produce failure in the analysis were much smaller than the actual peak value obtained in two tests. For a slope that resembles a flexible gravity wall, the

Fig. 9. Excavated section: Test 5 (PGA = 205% of Kobe's).

seismic reduction factor, RFs, needed to render failure is about 0.4. For a slope with narrow geocell facing and horizontal reinforcement extending backward into the backfill, the seismic reduction factor, RFs, is about 0.3. The FHWA (2001) guidelines for reinforced steep slopes allow for RFs of 0.5. Hence, compared with this work, the FHWA recommendation is somewhat conservative. The IITK (2005) recommendation for unreinforced slopes of 1/3 is amazingly close to the measured results.

Tests 1 and 3 show that gravity walls made of geocell can perform well under seismic loading. Such gravity systems may be economical for low walls. Test 5 shows that a reinforced slope, made entirely of geocell and soil, can be effective and likely economical.

It is noted that the term "failure" in this paper refers to a state where a fully formed slip surface within the soil mass is developed under seismic excitation. This state does not reflect catastrophic failures. Hence, the measured equivalent coefficients are likely conservative, as they do not represent failure in the sense of collapse. That is, these values represent an upper bound considering

a case where amplification of acceleration within the structure is insignificant, as was the case in the geocell tests. It is likely that the ductile nature of geocell reinforced slopes, where the reinforcement keeps the geometrical integrity of the structure while
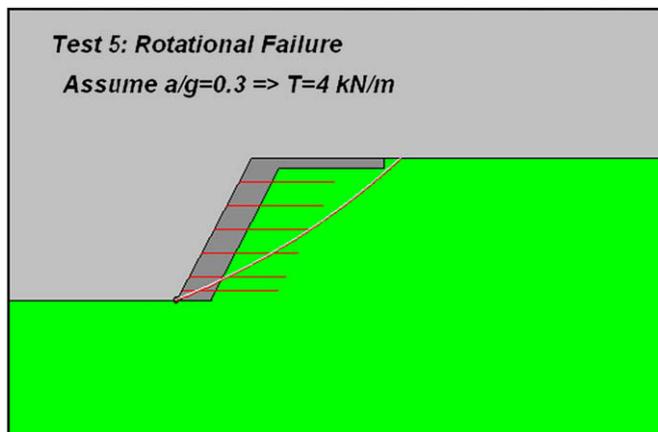

Fig. 10. Predicted slip circle for Test 5.

Fig. 11. Frontal view of wall in Test 3: post earthquake (159% of Kobe's PGA) – see excavated section of same wall in Fig. 3.

allowing for momentary large movements, may have only small amplification even at taller slopes than those tested.

The alternative approach of explicitly calculating permanent seismic displacement is briefly mentioned in Section 1 of this paper. Specifically, the "slip–stick" approach by Newmark (1965) is cited. A key parameter in the application of Newmark's approach is the yield acceleration which is determined from a pseudostatic LE analysis. Therefore, this paper is also relevant in the context of Newmark's approach.

Finally, a cautionary comment should be made about the results of this work in the context of design. All tests reported here included exposed geocell surface. Test 5 also used geocell layers as reinforcement elements. Current available geocells in the market are made of HDPE membrane strips welded to form 'honeycomb' 3-D geometry. Such membranes have high thermal coefficient resulting in large expansion and contraction of the geocell exposed to air and sun. Fluctuation in the geometry of the outer cells may result in progressively increasing stresses in the cell material potentially leading to its rupture. Furthermore, stress cracking at the exposed end could occur with low temperature. Ultraviolet degradation of the portion exposed to the sun could also be a concern. The end result could be a structure that deteriorates progressively, starting at the exposed face, having a lifespan shorter than desired. Equally important, when using a material made of HDPE membrane as reinforcement, its long-term strength would be very small. That is, the short-term strength must be reduced in design to account for creep rupture and ensure limited elongation (say, 5–10%) under the design load of the reinforcement. Since the tests reported here were conducted on virgin material under rapid loading condition, the long-term aspects of polymeric material as related to durability and capacity are not relevant. However, these aspects must be accounted for when extrapolating the results to design actual structures.

Acknowledgment

References

Ashford, S.A., Sitar, N., 2002. Simplified method for evaluating seismic stability of steep slopes. ASCE Journal of Geotechnical and Geoenvironmental Engineering 128 (2), 119–128.

Baker, R., Leshchinsky, D., 2001. Spatial distributions of safety factors. ASCE Journal of Geotechnical and Geoenvironmental Engineering 127 (2), 135–145.

FHWA, 2001. Mechanically Stabilized Earth Walls and Reinforced Soil Slopes Design and Construction Guidelines, Publication No. FHWA-NHI-00–043, Authored by Elias, V., Christopher, B.R., Berg, R.R.

Hynes-Griffin, M.E., Franklin, A.G., 1984. Rationalizing the Seismic Coefficient Method. Miscellaneous Paper GL-84-13. US Army COE, WES, Vicksburg, MS (citation taken from Kramer, 1996).

IITK, 2005. IITK-GSDMA Guidelines for Seismic Design of Earth Dams and Embankments. Prepared by Roy, Dayal, Jain. Indian Institute of Technology Kanpur and Gujarat State Disaster Mitigation Authority.

Kramer, S.L., 1996. Geotechnical Earthquake Engineering. Prentice-Hall, 653 pp.

Leshchinsky, D., Han, J., 2004. Geosynthetic reinforced multitiered walls. ASCE Journal of Geotechnical and Geoenvironmental Engineering 130 (12), 1225–1235.

Ling, H.I., Leshchinsky, D., 1998. Effects of vertical acceleration on seismic design of geosynthetic-reinforced soil structures. Geotechnique 48 (3), 347–373.

Ling, H.I., Mohri, Y., Leshchinsky, D., Burke, C., Matsushima, K., Liu, H., 2005. Large-scale shaking table tests on modular-block reinforced soil retaining wall. ASCE Journal of Geotechnical and Geoenvironmental Engineering 131 (4), 465–476.

Ling, H.I., Leshchinsky, D., Wang, J.P., Mohri, Y., Rosen, A. Seismic response of geocell retaining walls: experimental studies. ASCE Journal of Geotechnical and Geoenvironmental Engineering, in press.

Newmark, N., 1965. Effects of earthquakes on dams and embankments. Geotechnique 15 (2), 139–160.

Tatsuoka, F., Tateyama, M., Koseki, J., 1995. Behavior of geogrid-reinforced soil retaining walls during the Great Hanshin–Awaji earthquake. In: Ishihara, K. (Ed.), Proceedings of the First International Symposium on Earthquake Geotechnical Engineering, Balkema, Rotterdam, the Netherlands, pp. 55–60.